

THE ROLE OF DEFORMATION IN THE FORMATION  
OF METAMORPHIC GRADIENTS: RIDGE  
SUBDUCTION BENEATH THE OMAN OPHIOLITE

Bradley R. Hacker

Department of Geology, Stanford University, Stanford,  
California

*Abstract.* Two tectonic scenarios have been proposed for genesis and emplacement of the Oman ophiolite. One suggests that the ophiolite was generated at a spreading center, the other suggests generation within an intraoceanic arc. An integrated thermal and kinematic model of the temperature, stress, rock type, and displacement fields during early stages of the emplacement of the Oman ophiolite was developed to test these two possibilities. The thermal evolution was calculated by a finite difference algorithm for heat conduction, considering heats of metamorphic reactions, deformational heating, heat advection by flowing rock, mantle heat flow, and radioactive heating. The stress and displacement fields were calculated by an analytical model using a velocity boundary condition, power law constitutive relations, and a brittle frictional sliding relationship. Field observations in Oman can be satisfied with the spreading center model but not with the arc model. Moreover, simulations indicate that the ophiolite was probably <2 m.y. old at the time of intraoceanic thrusting and that shear stresses of ~100 MPa were attained during thrusting. In addition to satisfying currently available field constraints, these simulations also indicate specific further work that will help resolve the controversy over the evolution of this unique orogen. Future work should be directed toward (1) using thermobarometry and thermochronology to constrain the spatial variation in PTt paths of the metamorphic sole; (2) dating the igneous genesis of the ophiolite; and (3) using quartzite and dunite recrystallized grain size paleopiezometers to infer stresses during thrusting. These

simulations point out the important effect synmetamorphic deformation can have on the formation of metamorphic field gradients. In contractional fault zones, metamorphic field gradients may be normal or inverted and contracted or extended relative to the initial thermobarometric gradient, and adjacent fault zone rocks may display crossing PT paths. Unusually contracted or extended metamorphic field gradients may also develop in the footwalls of normal fault zones where portions of the hanging wall accrete to the uplifting, cooling footwall.

#### INTRODUCTION

The mechanisms by which slabs of oceanic lithosphere tens of thousands of square kilometers in area and as much as 20 km thick are emplaced onto less dense continental crust remain obscure. Tethyan-type ophiolites are emplaced onto continental margins by subduction of the edge of a continent beneath oceanic lithosphere [e.g., Moores, 1982], but the evolution of the deformation and metamorphism in such a convergence zone is poorly understood. Many ophiolite slabs are bounded below by soles, or basal fault zones, which consist of high-temperature metamorphic rocks. These soles accrete to the base of Tethyan-type ophiolites because the fault zone at the base of the ophiolite moves progressively downward in response to the cooling (and hardening) of the ophiolite peridotite and the heating (and softening) of the mafic rocks subducted beneath the ophiolite [Pavlis, 1986; Peacock, 1987; Hacker, 1990]. They contain inverted metamorphic field gradients more extreme than  $1000 \text{ K km}^{-1}$ , grading from mylonitic peridotite downward through granulite-, amphibolite-, and greenschist-facies rocks into unmetamorphosed material. These soles provide the key to understanding ophiolite emplacement because their metamorphic minerals and textures record their metamorphic and deformational history. Hacker [1990] presented

Copyright 1991  
by the American Geophysical Union

Paper number 90TC02779.  
0278-7407/91/90TC-02779\$10.00

simulations of the early stages of the thermal and kinematic history of the sole of the Oman ophiolite based specifically on the ophiolite emplacement hypothesis of Lippard et al. [1986]. It was concluded that Lippard et al.'s [1986] model, which considers the Oman ophiolite to have formed in an intraoceanic arc, is unable to explain several significant field observations in Oman. An alternative model wherein the Oman ophiolite formed at a mid-ocean spreading center, presented by Coleman [1981], Boudier and Coleman [1981], Boudier et al. [1988] and Montigny et al. [1988], is considered in this paper. For the purposes of this paper, a "metamorphic field gradient" is a gradient of (peak) metamorphic temperatures recorded in rocks, and a "thermal gradient" refers to an instantaneous gradient of temperatures in Earth at any given time [Spear and Peacock, 1989].

#### GEOLOGY OF THE OMAN OPHIOLITE

Most Tethyan ophiolites were emplaced onto the Afro-Arabian platform in Cretaceous time and then further deformed and metamorphosed during the continent-continent collision that ended the Alpine orogeny [Lippard et al., 1986]. The Oman ophiolite, however, was spared the continent-continent collision and constitutes a natural laboratory for investigating ophiolites. Diverse field studies of this complex have been published, including five journal issues or volumes dedicated to the Oman ophiolite [Glennie et al., 1974; Coleman and Hopson, 1981; Lippard et al., 1986; Boudier and Nicolas, 1988; Robertson et al., 1990b].

The Oman Mountains comprise a southwest directed system of oceanic thrust sheets (Figure 1) that were thrust over a Precambrian to Cretaceous continental autochthon in Cretaceous time and then overlapped by Maastrichtian and Tertiary sedimentary rocks. The autochthon includes continental shelf rocks of the Arabian platform resting on early Paleozoic and possibly late Proterozoic cratonal rocks [Glennie et al., 1974; Gass et al., 1990; Pallister et al., 1990]. The thrust sheets are, from structurally lowest (southwesternmost) to structurally highest (northeasternmost), the Sumeini Group, the Hawasina Complex, the Haybi Complex, the ophiolite, and the Batinah Complex. The Sumeini, Hawasina, and Haybi are continental slope, slope-basin, and seamount rocks, respectively, deposited in a Middle Triassic to Late Cretaceous passive margin and ocean basin northeast of the Arabian craton [Glennie et al., 1974; Woodcock and Robertson, 1982a; Lippard et al., 1986;

Béchenec et al., 1988; Robertson et al., 1990a]. The ophiolite, now disrupted into a number of relatively intact blocks, exposes a classic ophiolite pseudostratigraphy as recognized by the Penrose Conference Participants [1972]. The Batinah Complex includes mélangé believed to have been derived from beneath the ophiolite during late-stage extensional faulting and allochthonous thrust sheets of sedimentary rocks that slid onto the ophiolite late in the emplacement history [Woodcock and Robertson, 1982b; Robertson and Woodcock, 1983a].

The presently exposed ophiolite extends more than 600 km north-south, and is up to 150 km wide and 5–10 km thick. It is inferred to have been 16–20 km thick (Figure 2) prior to its dismemberment on the craton by extensional faulting. The ophiolite consists of a basal metamorphic sole (150–200 m), peridotite tectonite (8–12 km), igneous peridotite and gabbro (0.5–6.5 km), sheeted dikes (1–1.5 km), lavas (0.5–2.0 km), and overlying pelagic sedimentary rocks ( $\leq 100$  m) [Boudier and Coleman, 1981; Christensen and Smewing, 1981; Manghnani and Coleman, 1981; Pallister and Hopson, 1981; Lippard et al., 1986]. The metamorphic sole is the thrust zone at the base of the ophiolite and is composed of partially melted (rarely) lower granulite/upper amphibolite facies rocks at the top that grade downward into lower greenschist facies rocks. The majority of the amphibolites have trace element abundances that are intermediate between normal mid-ocean ridge basalts and within-plate tholeiites, similar to volcanic rocks in the underlying Haybi Complex [Searle and Malpas, 1980; Lippard et al., 1986]. The amphibolite-facies rocks are gneissic to schistose, and amphibole and plagioclase crystals contain crystal-plastic deformation features. Greenschist-facies rocks underlying the amphibolites include metamorphosed sandstone, shale, limestone, chert, and volcanic rocks, probably derived from the Hawasina Assemblage or the Haybi Complex. Initial metamorphism of the greenschist-facies rocks occurred during deformation, producing a penetrative schistosity, and later minerals grew during static conditions [Lippard et al., 1986]. The least disrupted exposures of the metamorphic rocks contain 60–100 m of amphibolite-facies rocks formed at peak temperatures ranging from 500° to 800°C and 80–120 m of greenschist-facies rocks formed at peak temperatures ranging from ~200°(?) to 500°C [Ghent and Stout, 1981; Searle and Malpas, 1982; Searle, 1990]. There are apparent discontinuities in metamorphic grade within the sole that indicate the presence of postmetamorphic faults, but the

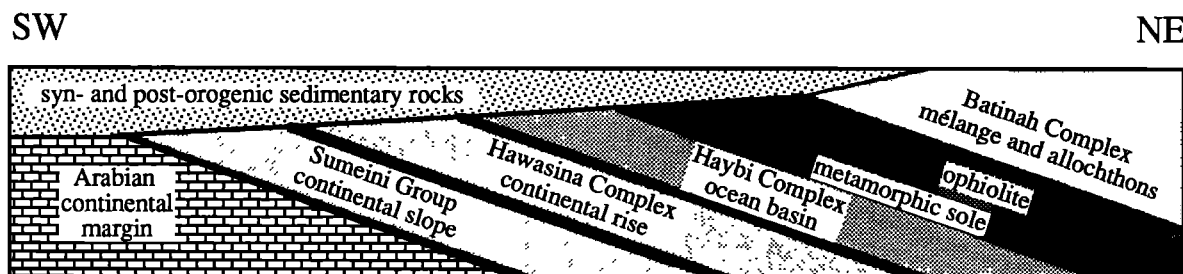


Fig. 1. Schematic illustration of the thrust sheets in the Oman Mountains.

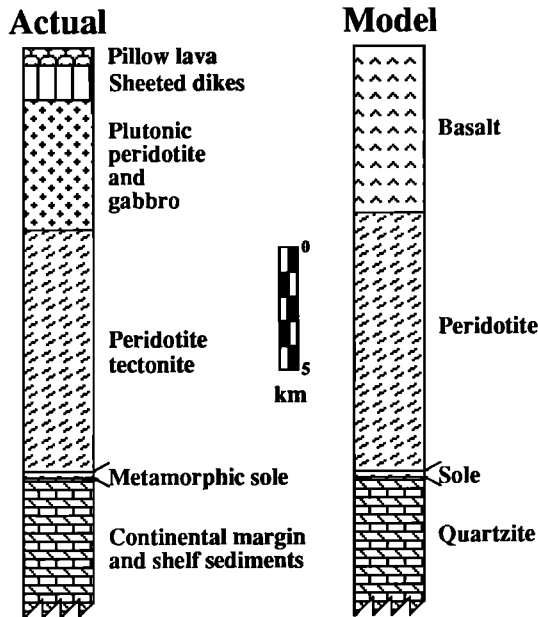


Fig. 2. A pseudostratigraphic section of the Oman ophiolite and underlying units and the simplified section used in the model. Sections measured in the field have 0.5–2.0 km of pillow lava, 1.0–1.5 km dikes, 0.5–6.5 km plutonic peridotite and gabbro, 8–12 km peridotite tectonite, and 0–0.2 km of metamorphic rocks [Boudier and Coleman, 1981; Christensen and Smewing, 1981; Manghnani and Coleman, 1981; Pallister and Hopson, 1981; Lippard et al., 1986]. The pseudostratigraphic section is a composite reconstruction based on numerous incomplete sections of variable thickness, and is inferred to represent the pseudostratigraphy of the ophiolite before disruption.

aforementioned thicknesses and temperatures imply metamorphic field gradients of  $>1000 \text{ K km}^{-1}$ . The amphibolite- and greenschist-facies rocks (Figure 3) yield K-Ar ages of ~100–70 Ma [Alleman and Peters, 1972; Searle et al., 1980; Lanphere, 1981; Montigny et al., 1988].

Two foliations have been mapped in the peridotite, (1) a pervasive coarse porphyroclastic foliation, and (2) a fine-grained porphyroclastic to mylonitic foliation in the lower 150–2000 m of the peridotite, which overprints the pervasive foliation and increases in intensity downward toward the metamorphic sole [Searle et al., 1980; Nicolas et al., 1980; Boudier and Coleman, 1981; Boudier et al., 1988; Ceuleneer et al., 1988]. The pervasive foliation is inferred to have formed during high-temperature, low-stress asthenospheric flow, and the mylonitic foliation is inferred to have formed at lower temperatures and higher stresses during emplacement of the ophiolite [Boudier and Coleman, 1981]. Olivine microstructures and two-pyroxene thermometry have been used to infer temperatures of mylonitization of 750°–1000°C [Boudier and Coleman, 1981; Lippard, et al., 1986; Ceuleneer et al., 1988].

The peridotite tectonite, igneous peridotite and gabbro, sheeted dikes, and lowermost lavas represent oceanic

lithosphere of “normal” chemistry and thickness [Alabaster et al., 1982; Pallister and Gregory, 1983; Lippard et al., 1986; Ernewein et al., 1988]. Eleven  $^{206}\text{Pb}$ - $^{238}\text{U}$  ages on plagiogranites in the intrusive sequence are in the range 95.4–93.5 Ma, although there are two that are slightly older (96.9 and 97.3 Ma); all ages have estimated uncertainties of  $\pm 0.5$  m.y. [Tilton et al., 1981]. The lowermost, oldest lavas may be cogenetic with the underlying sheeted dikes, whereas younger lavas have trace element affinities with island arc tholeiites [Lippard et al., 1986; Ernewein et al., 1988]. Pearce et al. [1981] and Alabaster et al. [1982] suggest that the younger lavas erupted above a subduction zone. Ernewein et al. [1988], however, point out that pelagic, not volcanoclastic, sedimentary rocks are interbedded with the younger lavas and prefer the interpretation that the lavas inherited their subduction zone component from either a regional mantle chemical anomaly or from second-stage melting of their mantle source. This is a critical difference because Pearce et al. [1981] and Lippard et al. [1986] interpret the Oman ophiolite as part of an arc that formed above an intraoceanic subduction zone, whereas Boudier and Coleman [1981], Coleman [1981], Ernewein et al. [1988], Montigny et al. [1988], Nicolas et al. [1988], Boudier et al. [1988], and Thomas et al. [1988] believe that the ophiolite was generated at a mid-ocean spreading center.

Hacker [1990] reported simulations of the formation of the sole of the Oman ophiolite based on the “arc” model proposed by Lippard et al. [1986]. The age of the ophiolite was assumed to be 5 m.y. at the inception of subduction, and the effects of subducting 5- to 100-m.y.-old lithosphere beneath the ophiolite were examined. The subduction zone was assumed to dip 45° to a depth of ~17 km, where the dip changed to horizontal. None of the simulations was able to reproduce either the peak metamorphic temperatures inferred for the Oman sole [Ghent and Stout, 1981; Searle, 1990], or the wide range of K/Ar ages reported for the metamorphic sole [e.g., Montigny et al., 1988].

One salient feature of the previous study [Hacker, 1990] is that the accretion of metamorphic rocks at the base of the Oman ophiolite can be explained with a transient, two-

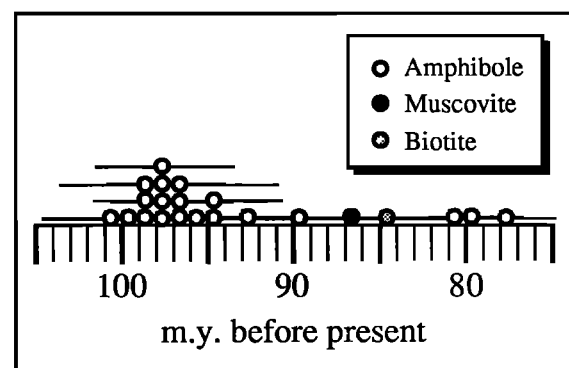


Fig. 3. K-Ar ages from the metamorphic sole of the Oman ophiolite from Alleman and Peters [1972], Lanphere [1981], and Montigny et al. [1988]. Mean values and 1 $\sigma$  standard deviations (horizontal bars) are shown.

dimensional thermomechanical model using laboratory measurements of the thermal and mechanical properties of rocks. Figure 4 illustrates the importance of this synmetamorphic faulting, using a conceptually simplified one-dimensional approach for ease of illustration. It shows a fault zone between two moving plates, the upper plate

ophiolite and the lower subducted plate. Consider a one-dimensional column through both plates (Figure 4a). The initial thermal gradient is a sawtooth, and deformation occurs at the base of the peridotite where the peridotite deforms by power law creep at stresses lower than those required for frictional sliding. As thermal conduction occurs, the thermal

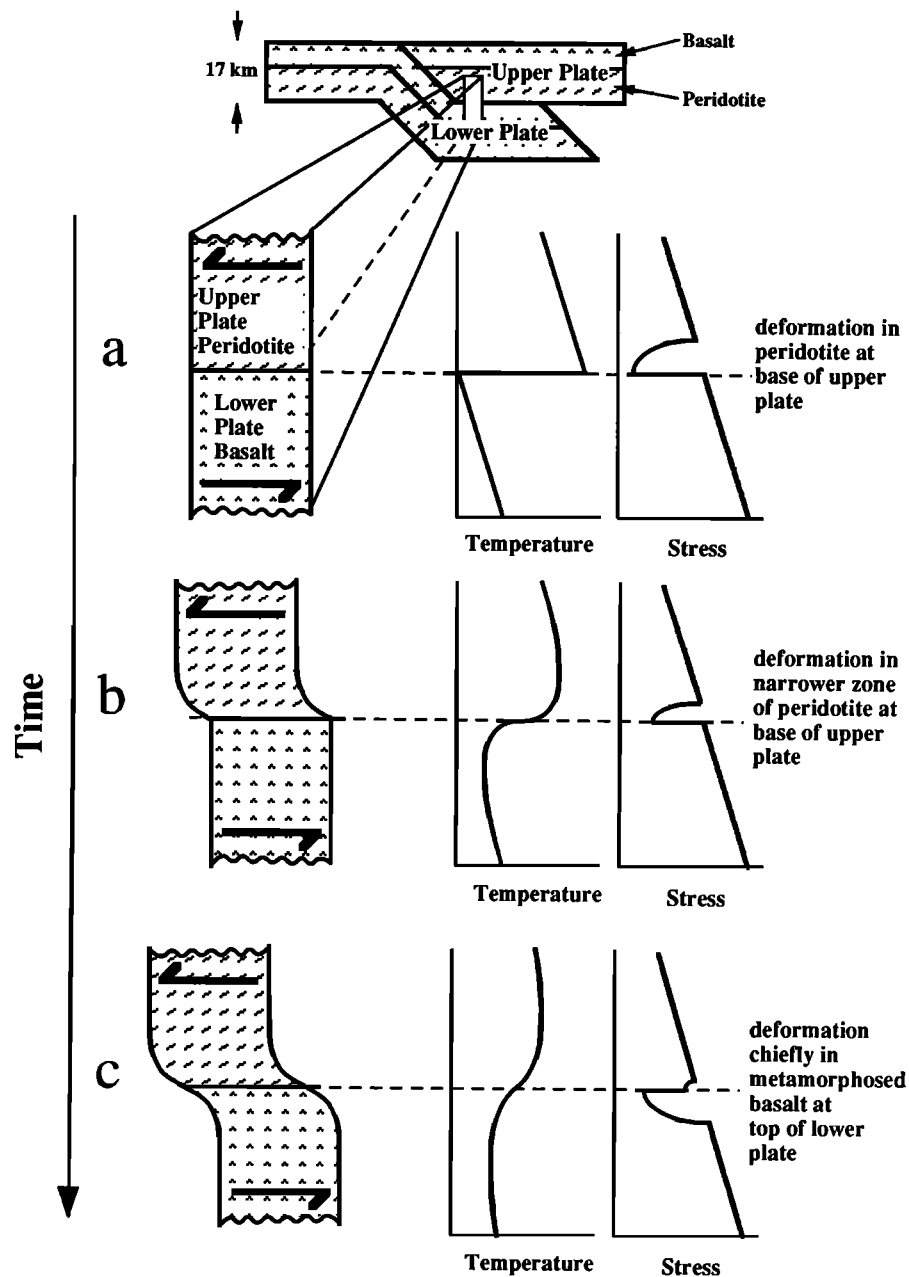


Fig. 4. One-dimensional cartoon of how conductive decay of a sawtooth-shaped thermal gradient can produce localized deformation at progressively deeper levels, resulting in accretion of metamorphic rocks to the base of the ophiolite. (a)-(c) Steps in a time sequence. Note that the simulations are not one-dimensional with a sawtooth thermal gradient but are two dimensional and consider time-dependent evolution of temperature and faulting.

gradient relaxes, and the upper portion of the lower plate basaltic layer is metamorphosed to greenschist facies (Figure 4b). The stress supported during power law creep of greenschist is greater than the stress for frictional sliding, so deformation continues only in the upper plate peridotite, although cooling of the upper plate causes the deformation to be concentrated in a narrower band. At a later time the lower plate reaches amphibolite-facies conditions and is then warm enough for power law creep to occur at stresses lower than those for frictional sliding and lower than those for power law creep of peridotite (Figure 4c). In these three steps, the zone of deformation moved progressively downward into the warming lower plate, and upper parts of the lower plate basaltic layer successively accreted to the base of the ophiolite.

This paper addresses the possibility that the Oman ophiolite represents the northeast flank of a mid-ocean spreading center. The important differences between this study and the previous one [Hacker, 1990] are that the possibilities of subduction of very young crust and subduction at a shallow angle ( $10^\circ$ ) are considered. The simulations successfully reproduce both the peak metamorphic temperatures inferred for the Oman sole and the wide range of K/Ar ages reported for the Oman sole. They suggest that the Oman ophiolite likely originated in oceanic lithosphere less than 2 m.y. old, and that shear stresses of  $\sim 100$  MPa were attained within the subduction zone.

## TECTONIC EVOLUTION OF THE OMAN OPHIOLITE

The field observations described above suggest the following tectonic evolution of the Oman ophiolite. In Late Permian time a passive margin formed on the Arabian platform [Blendinger et al., 1990]. Rifting of the basin and subsequent creation of new oceanic lithosphere resulted in terrigenous turbidite deposition succeeded by Middle Jurassic calcareous turbidite and chert deposition [Robertson and Searle, 1990]. In Late Jurassic to Early Cretaceous time, slow pelagic sedimentation was dominant. Radical change occurred in Albian to Cenomanian time, when intraoceanic subduction was initiated between  $\sim 101$  and 95 Ma. Metamorphism in the ophiolite sole spanned Albian to Campanian time (101–70 Ma); the amphibolite-facies metamorphism occurred between 101 and 89 Ma, and the greenschist-facies rocks developed from 87 to 76 Ma. During this interval, the allochthonous plates were assembled and faulted onto the Arabian continental margin. By Maastrichtian time (70–65 Ma) all the plates had been partially eroded and transgressed by shallow-water carbonate rocks. These parts of the ophiolite development are agreed upon by most authors [Lippard et al., 1986; Boudier and Nicolas, 1988]. However, as mentioned previously, there is disagreement regarding the petrogenesis and tectonic implications of the younger lavas. Lippard et al. [1986; p. 155] suggest that the ophiolite evolved on the southwest flank of a backarc spreading center above a

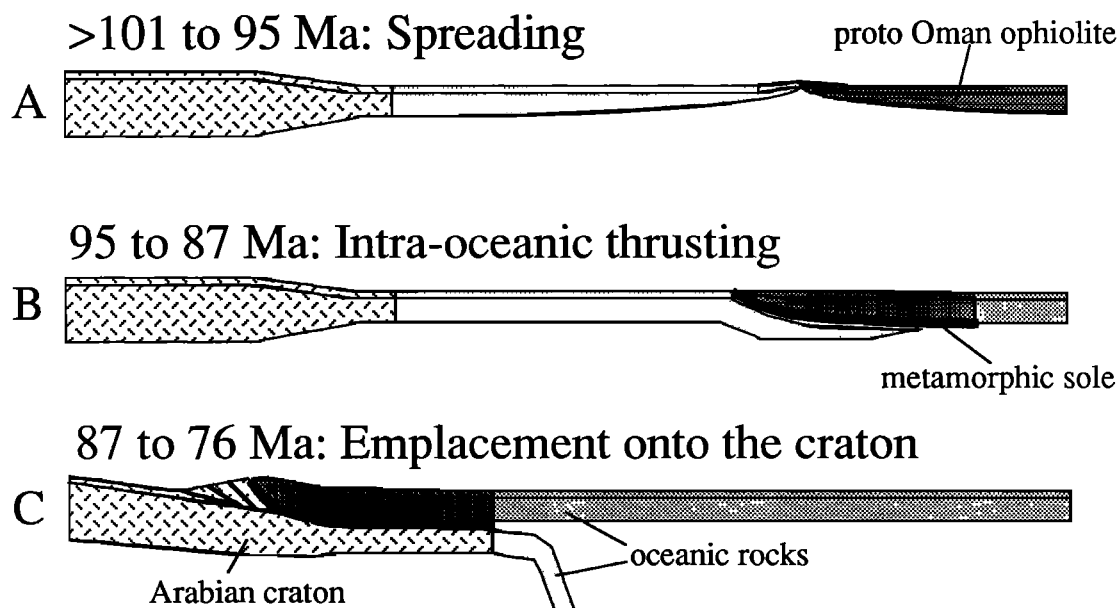


Fig. 5. Hypothetical palinspastic reconstruction of the genesis and emplacement of the Oman ophiolite [after Boudier and Coleman, 1981; Boudier et al., 1988; Montigny et al., 1988]. (a) Prior to 101–95 Ma: Spreading is active in the ocean basin; the two plates of oceanic crust are shown in different shades. (b) 95–87 Ma: The ophiolite is thrust over adjacent oceanic crustal rocks, which are accreted at amphibolite-facies conditions to the base of the ophiolite, shown by a heavy line. (c) 87–76 Ma: The ophiolite is thrust over continental rocks, which are accreted at greenschist-facies conditions to the base of the ophiolite.

subduction zone dipping away from the continent. They propose that the intraoceanic subduction initiated at the contact between the young crust and the older (5–100 m.y. older) oceanic lithosphere into which it was intruded. This possibility was addressed in a previous study [Hacker, 1990]. In contrast, Boudier and Coleman [1981], Montigny et al. [1988; p. 359], Ernwein et al. [1988; p. 270], Nicolas et al. [1988; p. 51], Boudier et al. [1988; p.289], and Thomas et al. [1988; p. 318] suggest that the ophiolite originated on the northeast flank of a mid-ocean spreading center and that intraoceanic subduction was initiated at the ridge axis (Figure 5). It is this “ridge” model that is addressed in the current study.

According to the Ernwein et al. [1988] model the absence of arc rocks in the ophiolite seems to conflict with the inference that the ophiolite formed in an ocean basin with a half width of ~450 km [Béchenec et al., 1988]. For the ophiolite to have reached the craton, the 450 km of oceanic lithosphere must have been subducted beneath the ophiolite, surely enough material could have melted to form a magmatic arc. There are at least two ways to reconcile these observations. If the subduction occurred at a shallow angle, melting may have been inhibited or have produced liquids unlike typical arc magmas [e.g., Lipman et al., 1971; Coney and Reynolds, 1977]. Alternatively, the 450 km of oceanic lithosphere may have been duplicated by thrusting before being subducted beneath the ophiolite, such that the effective width of the subducted lithosphere was much less than 450 km.

The suggestion that the Oman ophiolite came from the northeastern side of a northwest-southeast spreading ridge is based on the northeastward thickening taper of the slab [Lippard et al., 1986]. Other attempts to determine which flank of a spreading center is represented in Oman, based on dike chilling directions [Pallister, 1981; Lippard et al., 1986, p. 99], the inclination of cumulus layering in plutonic rocks [Pallister and Hopson, 1981], and the shear sense recorded in the mantle tectonite [Boudier and Coleman, 1981; Nicolas et al., 1988] yield equivocal results.

Various structural indicators have been used to infer the thrusting direction during emplacement of the Oman ophiolite. The structures are not uniform from one massif to another but in general indicate ridge-parallel movement in the mylonitic peridotite, and ridge-orthogonal movement in the metamorphic sole [Boudier et al., 1988; Thomas et al., 1988]. Paleomagnetic data [Thomas et al., 1988] indicate that the various massifs of the Oman ophiolite have not rotated significantly with respect to one another, so these variations in thrusting direction represent spatial variation in the emplacement direction.

Paleomagnetic data also allow Thomas et al. [1988] to suggest that the ophiolite was created at a northeast trending spreading center, was rotated 75° counterclockwise soon thereafter and was then rotated 40° clockwise before emplacement onto the Arabian craton. Together with the paleomagnetic data the vergence directions indicate that the Oman ophiolite always moved toward the southwest: initial movement recorded by the peridotite was parallel to the ridge (toward the southwest), and later movement recorded by the metamorphic sole was perpendicular to the ridge (also

toward the southwest), following rotation of ~75° counterclockwise [Thomas et al., 1988].

## MODEL

A thermomechanical model developed previously [Hacker, 1990] to test part of the arc tectonic model proposed by Lippard et al. [1986], is used in this study to test part of the ridge tectonic model proposed by Boudier and Coleman [1981], Boudier et al. [1988] and Montigny et al. [1988]. The model predicts the stress field, temperature field, rock type, and displacement field histories during the early stages of the ophiolite emplacement process, and these predictions are then shown to compare favorably with field observations. Later stages of the emplacement process, which may have involved gravity sliding, are not modeled. Boudier et al. [1988] and Montigny et al. [1988] propose that spreading at a mid-ocean ridge formed the Oman ophiolite (Figure 5a). Later, at ~101–95 Ma, subduction began along the spreading axis (Figure 5b). Basaltic rocks from the underthrust plate were metamorphosed at amphibolite-facies conditions and accreted to the base of the ophiolite (Figure 5b) from 101 to 89 Ma, and then continental material was accreted to the sole at greenschist-facies conditions from 87 to 76 Ma (Figure 5c). The convergence velocity was assumed to be 50 mm yr<sup>-1</sup> [Boudier et al., 1988, Figure 12], although the effects of variations in this rate were also investigated. The rate of subduction must have been at least 25 mm yr<sup>-1</sup>, because ~630 km of oceanic and continental lithosphere were subducted beneath the ophiolite in ~25 m.y. Convergence parallel and perpendicular to the ridge axis was tested. The total amount of oceanic lithosphere subducted beneath the ophiolite is estimated very roughly as ~450 km by palinspastic reconstruction of basinal rocks [Glennie et al., 1974; Lippard et al., 1986; Béchenec et al., 1988; Cooper, 1988]. The total amount of continental lithosphere subducted is estimated as 180 km, from the width of the ophiolite outcrop on the Arabian craton. The subducted oceanic lithosphere was a few million years old at the time of subduction, and probably developed at rates >10–20 mm yr<sup>-1</sup> [Boudier et al., 1988], perhaps up to 50 mm yr<sup>-1</sup> [Pallister and Hopson, 1981; Nicolas et al., 1988]. The convergence velocity was assumed to be 50 mm yr<sup>-1</sup> in the simulations. The subducted continental lithosphere was ~720–760 m.y. old [Glennie et al., 1974; Gass et al., 1990; Pallister et al., 1990].

The angle of subduction in the simulations (10°) was taken to be constant with depth; note that this is different from the geometry assumed by Hacker [1990], where the subduction occurred at 45° to a depth of ~17 km, and then was horizontal. It has been suggested by Boudier et al. [1985; 1988] that the dip of the subduction zone can be inferred from the wedge shape of the Oman ophiolite. Boudier et al. [1988] state that field observations suggest that the dip of the subduction zone was 2°–3°, however, published cross sections do not concur with this figure. The ophiolite slab thickens northeastward from 2–4 km thick in Bahla to 10–12 km thick in Rustaq, 37–72 km away [Boudier et al., 1988], indicating a dip of 5°–15°. In the Wadi Tayin massif a thickness change of 3.7 km occurs over a distance of 28.6 km, indicating a taper of 7.4° [Boudier and Michard, 1981; Boudier et al., 1988; Figure 2a].

Moreover, gravity modeling of Shelton [1990] shows a wedge-shaped slab with an angle of  $\sim 11^\circ$ . Thus a subduction zone dip of  $10^\circ$  was chosen for the present study.

Subduction zones formed in young oceanic lithosphere are expected to be inclined at shallow angles because of the low density of young lithosphere. Turcotte et al. [1977] calculated that several hundred kilometers of oceanic lithosphere must be overridden by material of mantle density before (steep) subduction can be initiated because of the flexural strength of the lithosphere. Sacks [1983] showed that subducted lithosphere  $\leq 20$  m.y. old is buoyant within asthenosphere and will subduct subhorizontally beneath an overriding plate.

#### Thermal Model

Calculations were made for a cross section 34 km thick and 100 km long (Figure 6). The upper plate ophiolite occupied roughly the upper right portion of this area, and the lower plate subducted material began to the left and was subducted beneath the upper plate. The cross section was divided into nodes spaced 1 km vertically and 2 km horizontally. In a 1-km-thick region above and below the subduction zone the vertical node spacing was reduced to 100 m so that more detailed information could be collected in the fault zone.

The thermal evolution was evaluated by solving the conservation of energy equation with a two-dimensional alternating direction implicit finite difference algorithm. Heat conduction, heats of metamorphic reactions, deformational heating, radioactive heat production in continental crust, advection of heat by rock displacement were taken into account, whereas kinetic energy and adiabatic compression were neglected. During subduction, heat was allowed to advect but not conduct through the ends of the model. After subduction, erosion and heat flow from the mantle were considered.

The temperature field at the initiation of each simulation was calculated after Parsons and Sclater [1971] and depends only on the age of the lithosphere and the peridotite solidus

(Figure 6). Kusznr [1980], Bratt et al. [1985], and Morton and Sleep [1985] have developed models of the cooling of oceanic lithosphere that attempt to account for the effects of hydrothermal circulation, latent heat of crystallization, and the presence of discrete magma chambers. Their preferred models are not significantly different than the model used in this study for lithosphere ages as young as 0.1 m.y., which is the youngest age considered here. The thermal gradient within the continental lithosphere was calculated using heat flow and heat production values for the Appalachian orogen of the United States [Morgan, 1984], a passive margin for approximately the same duration as the Arabian craton.

#### Rock Types

For the purpose of modeling, the pseudostratigraphy of the ophiolite (Figures 2 and 6) was simplified to a 7-km basaltic layer and a 10-km peridotite layer. Because of small thickness ( $< 100$  m), the pelagic sediments overlying the Oman ophiolite [Robertson and Woodcock, 1983b; Lippard et al., 1986] were ignored. The grid nodes in the basaltic layer were assumed to contain mineral assemblages appropriate to their pressure and temperature: either prehnite-pumpellyite, greenschist-, or amphibolite-facies minerals.

#### Thermal Parameters

The rocks were assigned a density of  $3000 \text{ kg m}^{-3}$ , a heat capacity of  $1200 \text{ J kg}^{-1} \text{ K}^{-1}$ , and a thermal conductivity of  $3 \text{ J K}^{-1} \text{ m}^{-1} \text{ s}^{-1}$ . The rock types change through metamorphic reactions, which release or consume heat. In the model the zeolite  $\leftrightarrow$  greenschist and greenschist  $\leftrightarrow$  amphibolite transitions occur instantaneously at  $250^\circ\text{C}$  and  $450^\circ\text{C}$ , respectively. A value of  $2.44 \times 10^8 \text{ J m}^{-3}$  was used for the dehydration of zeolite-facies rocks, and  $1.2 \times 10^8 \text{ J m}^{-3}$  for dehydration of greenschist-facies rocks to form amphibolite. For a discussion of the selection of these values and an evaluation of the effects of their uncertainties, see Hacker [1990].

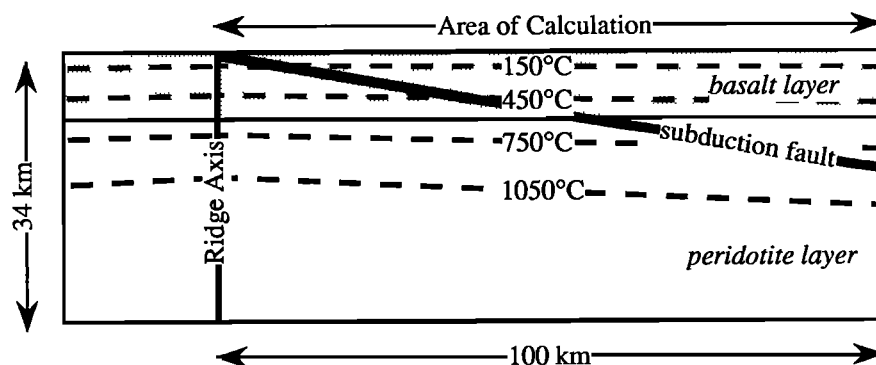


Fig. 6. Initial conditions of a simulation where 2-m.y.-old lithosphere formed at  $50 \text{ mm yr}^{-1}$  is subducted beneath 2-m.y.-old lithosphere formed at the same rate. The plate on the left represents the lithosphere to be subducted beneath the plate on the right. The heavy diagonal line marks the predefined  $10^\circ$  trace of the subduction zone.

### Mechanical Parameters

The stress and displacement fields were calculated with an analytical model using velocity boundary conditions, temperature-dependent power law constitutive relations, and a pressure-dependent brittle frictional sliding relationship. The horizontal velocity boundary condition specifies the rate at which material is subducted beneath the ophiolite. The stress estimate is the result of the velocity boundary condition and the rheology of the rocks. The displacement field defines the advection and determines where the deformation occurs.

The strength of rock was computed as a function of pressure, temperature, strain rate, and rock type. Three modes of deformation were considered: (1) brittle frictional sliding, (2) power law creep, and (3) transitional behavior (Figure 7). Whichever mode of deformation required the lowest stress at a given node (i.e., at a given pressure, temperature, and rock

type), was considered to be the only active mode of deformation at that node. At low temperatures and pressures, brittle failure occurs because power law creep strengths are large at low temperatures, whereas the brittle strength is small at low pressures and assumed to be independent of temperature. Fluid pressure was assumed to be hydrostatic. At high temperatures and pressures, power law creep occurs because the brittle strength is large at high pressures, whereas power law creep strengths are low at high temperatures and assumed to be independent of pressure. See Hacker [1990] for a discussion of the selection of these values, and an evaluation of the effects of their uncertainties.

### Calculation Procedures

A time step of 0.01 m.y. was used to ensure stability of the thermal calculations. Each time step was composed of the following:

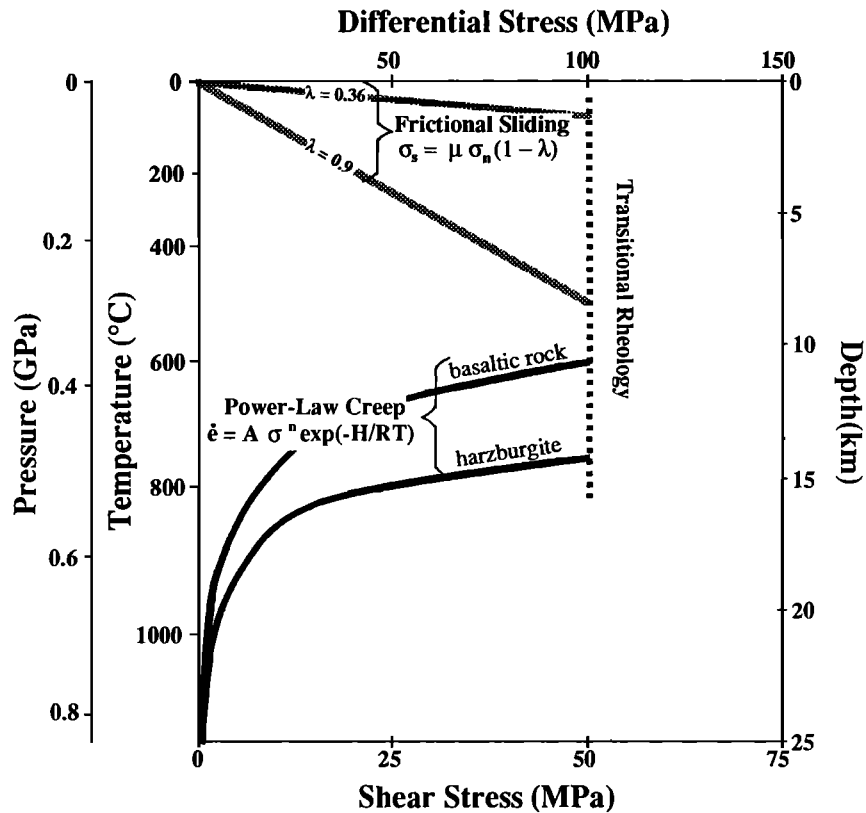


Fig. 7. Strength was determined as a function of pressure, temperature, and rock type. At shallow depths, low pressures, and low temperatures, frictional sliding occurs; the strength was determined by a relationship of the form:  $\sigma_s = \mu \sigma_n (1 - \lambda)$  (pressures are shown on the vertical axis, and the strain rate is  $10^{-12} \text{ s}^{-1}$ ). At great depths, high pressures, and high temperatures, power law creep occurs; the strength was determined by a relationship of the form:  $\dot{\epsilon} = A \sigma^n \exp(-H/RT)$  or  $\sigma = (\dot{\epsilon}/(A \exp(-H/RT)))^{1/n}$  (temperatures are shown on the vertical axis). A transitional regime occurs at intermediate depths where the frictional sliding and power law creep strengths exceed 200 MPa differential stress.  $\lambda$ , pore pressure fraction of total pressure;  $\sigma_s$ , shear traction;  $\mu$ , friction;  $\sigma_n$ , normal traction;  $\dot{\epsilon}$ , strain rate;  $A$ , pre-exponential constant;  $\sigma$ , differential stress;  $n$ , stress exponent;  $H$ , activation enthalpy;  $R$ , gas constant;  $T$ , absolute temperature. Thermobarometric gradient shown applies to oceanic lithosphere of  $\sim 5$  m.y. age.

1. Determine where any metamorphic reactions occur. Change rock types as appropriate, and add or subtract heat.
2. Allow heat to conduct.
3. Calculate the differential stress in each column that sustains the imposed horizontal velocity boundary condition.
4. Compute the resultant vertical gradient in the horizontal strain rate and displacement in each column.
5. Determine the amount of heat generated by deformational heating.
6. Move material to reflect the displacement gradient in each column.
7. Return to step 1.

The simulations were halted when 450 km of oceanic lithosphere and 180 km of continental lithosphere had been subducted beneath the ophiolite. The small time step means that the calculations are implicitly self-consistent (e.g., the correct interplay between deformational heating and stress is effectively maintained by iteration on a 0.01 m.y. time step).

## RESULTS

Many simulations were conducted using the tectonic history suggested by Boudier and Coleman [1981], Boudier et al. [1988] and Montigny et al. [1988]. The influence of model parameters was evaluated by varying the value of each parameter while holding all other parameters constant. Specifically, a range of values for lithosphere age, subduction velocity, thermal conductivity, and maximum stress were examined. The effects of subduction parallel and perpendicular to the ridge axis were also considered.

Two disparate models with different lithosphere age and maximum stress are shown here. In both, subduction begins at a spreading center; the axis of the spreading center is at the left edge of Figures 8a and 9a. In Figure 8 the lithosphere is 2 m.y. old and the maximum shear stress is limited to 100 MPa. In Figure 9 the lithosphere is 0.1 m.y. old and the maximum shear stress is limited to 50 MPa.

Both simulations produce qualitatively similar results. Note that steady state is not achieved because the amount and distribution of deformational heating are constantly changing and the age of the subducted lithosphere is steadily increasing. Although there initially is less heat in the 2-m.y.-old lithosphere, the higher maximum stress produces more deformational heating, leading to greater isotherm overturn and longer retention of heat. The lower panel in each figure corresponds to when continental lithosphere begins to be subducted beneath the ophiolite.

A useful test of these simulations is to compare their predicted pressure-temperature paths with pressures and temperatures inferred from field studies in Oman. Figure 10 shows the pressure-temperature paths for various nodes that begin within the uppermost part of the lower plate and finish accreted to the base of the upper plate. Both figures show four pressure-temperature paths. The paths labeled "0 m.y." correspond to material subducted at the initiation of intraoceanic thrusting, whereas the "9 m.y." paths are for material subducted 9 m.y. after intraoceanic thrusting began. Because the subduction rate is 50 mm yr<sup>-1</sup>, these points were initially 450 km apart on the downgoing plate. The paths labeled "deep accretion" show pressure-temperature trajectories for material accreted at the inferred maximum

depth exposed in the metamorphic sole in Oman; whereas the "shallow accretion" paths show pressure-temperature trajectories for material accreted at shallower depths. Many other pressure-temperature paths are possible, but the maximum pressure may be constrained by the thickness of the ophiolite slab, and the maximum temperature can not be greater than the "deep accretion" path shown because material subducted to greater depths is not exposed in the metamorphic sole in Oman. The decompression and cooling paths depend on the simulated uplift history. The uplift history is not critical in this study because the ophiolite was lifted up and exposed so rapidly that little thermal overprinting of the sole rocks could have occurred; the ophiolite was subaerially exposed within 5–10 m.y. after the greenschist-facies metamorphism of the sole [Woodcock and Robertson, 1982b, p. 67]. Note that even higher pressures might have been attained if the upper plate were initially thicker and has been structurally thinned during subduction as suggested by Casey and Dewey [1984].

The box in Figure 10 shows the peak pressures and temperatures reached during amphibolite-facies metamorphism at the base of the Oman ophiolite, as estimated from thermobarometry [Ghent and Stout, 1981; Searle, 1990]. These peak metamorphic conditions are achieved in the simulation with 0.1-m.y. old lithosphere and a limit on the differential stress of 100 MPa (Figure 10b). The inferred metamorphic temperatures are almost reached in the simulation with 2-m.y. old lithosphere and a 200 MPa differential stress limit (Figure 10a). Simulations with lower limits on the stress or with older lithosphere reach lower peak temperatures. Figure 3 shows that most dated rocks in the Oman sole cooled through K/Ar hornblende closure temperatures [ $\sim 525 \pm 25^\circ\text{C}$ ; Harrison, 1981] over a period of  $\sim 7$  m.y. Both the simulations presented here sustain  $525 \pm 25^\circ\text{C}$  temperatures for  $\sim 6$ –9 m.y. Note that none of the simulations using a different subduction geometry presented in Hacker [1990] produced temperatures in accord with thermobarometric estimates or temperatures  $> 500^\circ\text{C}$  for  $> 2$ –3 m.y., although, there too, the highest temperatures were sustained longest in the younger subducted plate. The simulations presented here suggest that very young lithosphere supporting differential stresses of the order of 100 MPa are required to replicate field observations in Oman.

Because of the inverse nature of the approach used in this study, the predictions of the simulations are not necessarily unique and variables or processes not considered may play important, unrecognized roles. We can, however, evaluate the sensitivity of the models to parameters other than lithosphere age and maximum stress.

Increasing the subduction velocity reduces the time required to subduct a given amount of material. Consequently, heat advection gains importance relative to heat conduction. Thus for a given amount of subduction the thermal gradient between the two plates is more extreme when subduction is rapid and less so when subduction is slow. For a slow subduction velocity, heat in the upper plate is transferred more rapidly into the lower plate. Initially this causes more rapid metamorphism of the lower plate basaltic material and more rapid downward progression of the fault zone (i.e., accretion to form the sole). In the long term, however, thermal equilibration of the entire column causes

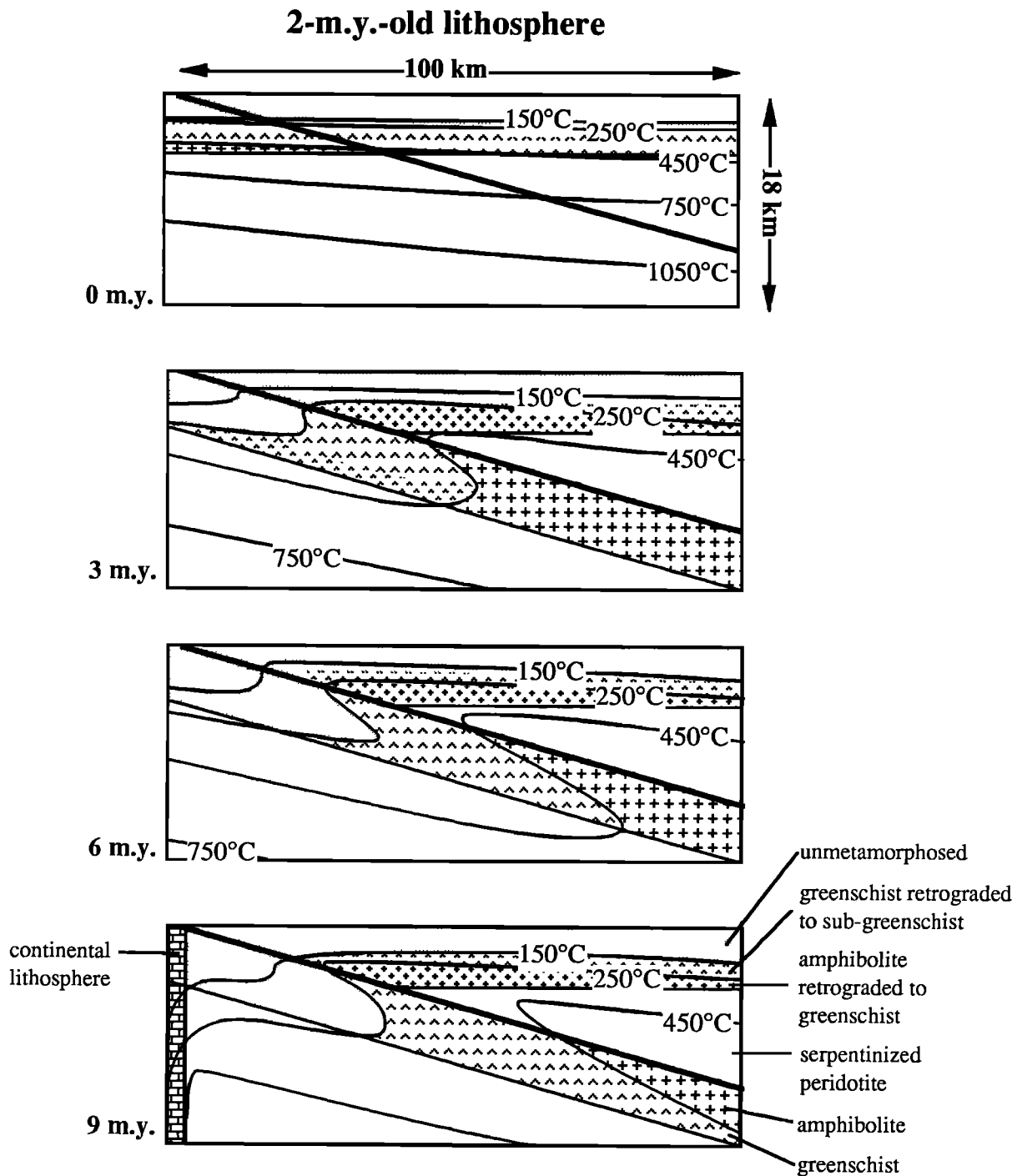


Fig. 8. A time sequence illustrating the temporal and spatial changes in temperatures and rock types calculated for 2-m.y.-old lithosphere (vertical exaggeration 2X). The maximum differential stress was 200 MPa. All material above the fault zone (heavy line) is the ophiolite.

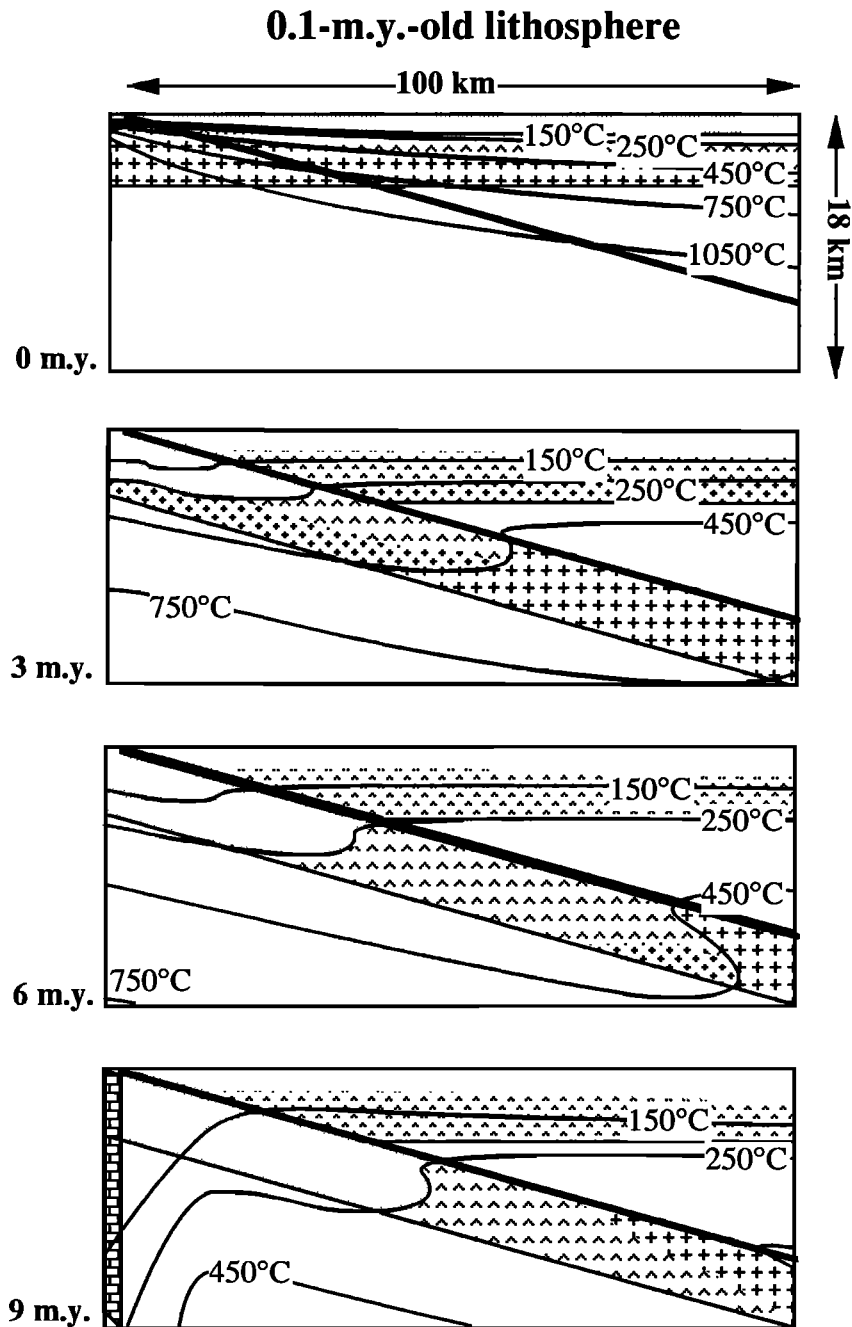


Fig. 9. A time sequence illustrating the temporal and spatial changes in temperatures and rock types calculated for 0.1-m.y.-old lithosphere (vertical exaggeration 2X). The maximum differential stress was 100 MPa. All material above the fault zone (heavy line) is the ophiolite.

the fault zone to cool to temperatures too low for dislocation creep and resetting of hornblende K/Ar systematics. Deformational heating is reduced during slower subduction, which also tends to reduce the lifetime of the system. For these reasons the peak temperatures obtained during slower subduction are lower than those during faster

subduction. Simulations with subduction rates of 50–100 mm yr<sup>-1</sup> produce peak temperatures compatible with those inferred from field studies [Ghent and Stout, 1981; Searle, 1990], while simulations with subduction rates as slow as 25 mm yr<sup>-1</sup> do not.

Increasing the thermal conductivity increases the rate of

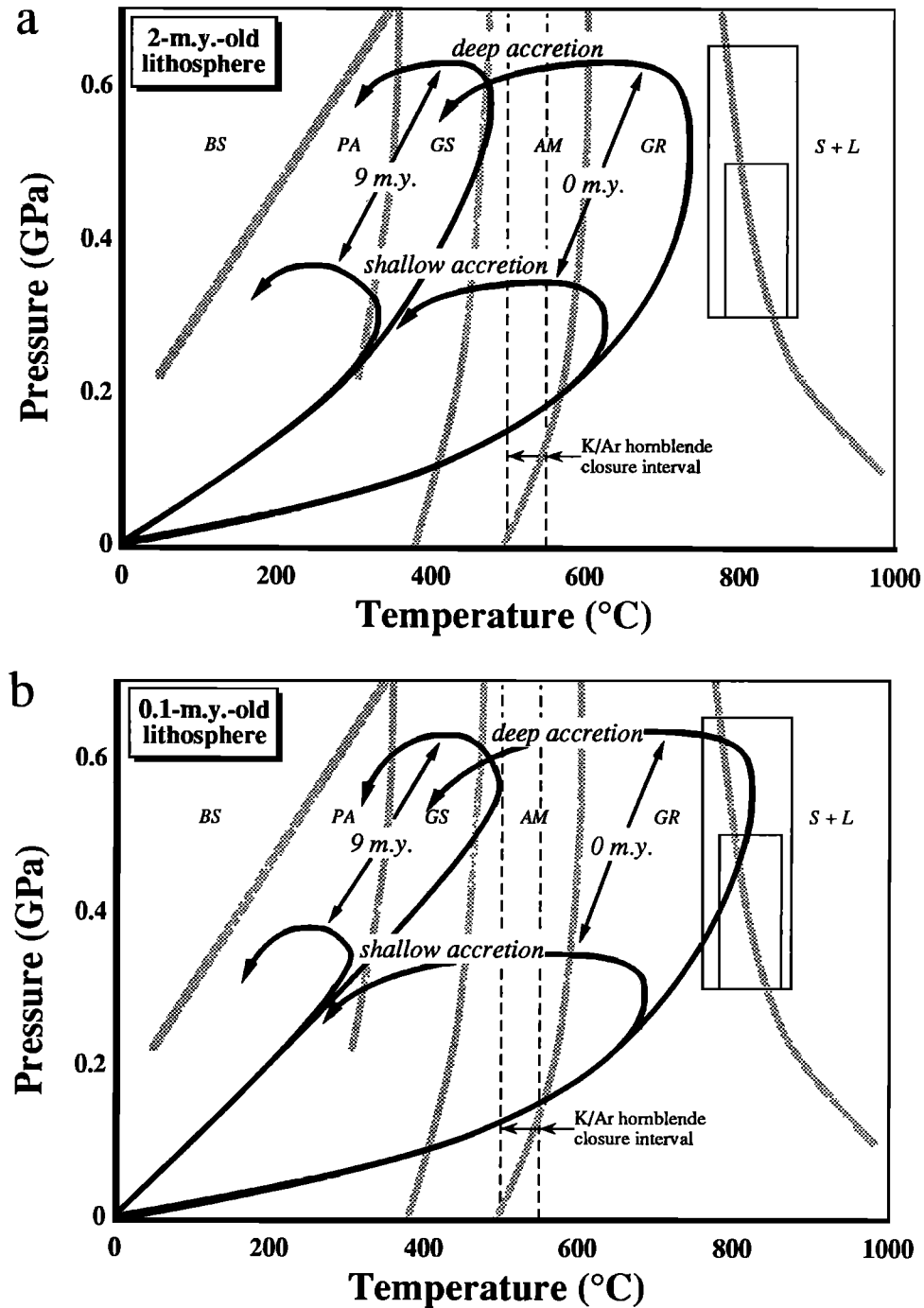


Fig. 10. Pressure-temperature paths for rocks accreted to the metamorphic sole at different times and depths. The rectangles illustrate peak pressures and temperatures estimated by Ghent and Stout [1981] and Searle [1990] for the amphibolite-facies mafic rocks in Oman. Dashed vertical lines show approximate K/Ar hornblende closure temperature interval [Harrison, 1981]. Shaded lines show metamorphic facies boundaries and a solidus. BS, blueschist facies; PA, pumpellyite-actinolite and prehnite-pumpellyite facies; GS, greenschist facies; AM, amphibolite facies; GR, granulite facies; S+L, region of partially melted rocks. (a) Lithosphere is 2 m.y. old and maximum differential stress is 200 MPa (corresponds to Figure 8). (b) Lithosphere is 0.1 m.y. old and maximum differential stress is 100 MPa (corresponds to Figure 9).

heat conduction. When the thermal conductivity is increased, the subducted plate heats up more rapidly, and the upper plate cools more rapidly. Consequently, the subducted basaltic rocks undergo prograde metamorphism more rapidly and support smaller stresses when deforming. This produces interesting feedback among deformational heating, heating through metamorphic reactions, and thermal conduction. Smaller stresses produce less deformational heating, and more rapid prograde metamorphism means more rapid consumption of heat by dehydration reactions, but in the simulations this is nearly compensated by the increased thermal conduction. These competing effects are so evenly balanced that it is not possible to discriminate among simulations with conductivities varying from 2 to 4 J K<sup>-1</sup> m<sup>-1</sup> s<sup>-1</sup>.

In simple terms, increasing the transitional stress increases the number of nodes that deform by frictional sliding or crystal plasticity. More importantly, a higher ceiling on the stress increases deformational heating, and this retards the rate at which the upper plate cools and speeds the rate at which the lower plate is heated. In simulations where the maximum shear stress was limited to 50 MPa the peak metamorphic temperatures estimated from field studies [Ghent and Stout, 1981; Searle, 1990] could only be obtained in simulations with oceanic lithosphere <0.1 m.y. old. Increasing the maximum shear stress limit to 100 MPa resulted in appropriate simulated peak temperatures for lithosphere <2 m.y. old. Deformational heating was much more important in this model than in the model of Hacker [1990] primarily because the velocity declined monotonically in the latter model, leading to decreasing deformational heating with time.

Paleomagnetic [Thomas et al., 1988] and structural data [Boudier et al., 1988] suggest that the initial movement of the ophiolite was parallel to the ridge and later movement was perpendicular to the ridge. Turcotte et al. [1977] showed through simple calculations that oceanic lithosphere younger than 6 m.y. is more buoyant than average mantle material and will not sink when it is overlain by average mantle, whereas lithosphere older than 6 m.y. is dense enough that it will. This may provide an explanation of why the change from ridge-parallel to ridge-orthogonal convergence occurred. During initial convergence the spreading center was younger than 6 m.y. and more buoyant than average mantle. Later, when the spreading center was older than 6 m.y., it was dense enough to sink beneath the overriding Oman ophiolite. Simulations of ridge-perpendicular subduction were also made and compared with the ridge-parallel simulations. The differences are small, and existing field data cannot be used to distinguish between the two.

In summary, variation of these key parameters suggests that the ophiolite and the material subducted beneath it were ≤2 m.y. old and that shear stresses reached ~100 MPa. There is one important reason why the ridge model is preferable to the arc model of Lippard et al. [1986]: the arc model requires that the lithosphere subducted beneath the ophiolite must be older than the ophiolite itself. If the ophiolite is 180 km wide and formed at rates of 20–50 mm yr<sup>-1</sup>, then the subducted lithosphere must have been 4–9 m.y. old at the initiation of subduction. The simulations presented here and

previously [Hacker, 1990] indicate that such old lithosphere does not contain enough heat to replicate the peak metamorphic temperatures recorded in Oman.

## DISCUSSION

The inverted metamorphic field gradients beneath ophiolites are much steeper than thermal gradients produced in thermal models of thrust faults. For example, Peacock [1987] modeled the thermal effects of fluid flow in subduction zones. Without including deformational heating he was able to produce inverted thermal gradients as steep as 123 K km<sup>-1</sup>, but no greater. Such gradients were produced in his models of very rapid subduction (100 mm yr<sup>-1</sup>) of very young (5 m.y.-old) lithosphere. Peacock [1987] further noted that deformational heating of >0.25 W m<sup>-2</sup> (equivalent to a shear stress of 160 MPa acting at subduction velocities of 50 mm yr<sup>-1</sup>) could generate gradients of 250 K km<sup>-1</sup>. The simulations in the present study also evolve thermal gradients of the order of 100 K km<sup>-1</sup>. Natural metamorphic soles beneath ophiolites have peak metamorphic temperature gradients of at least 1000 K km<sup>-1</sup> [Jamieson, 1986]. Why is it that models fail to produce thermal gradients as steep as natural metamorphic field gradients? The resolution to this apparent paradox is that the roles of accretion and structural erosion during subduction in the generation of metamorphic field gradients have not been taken into account. Downward accretion during subduction results in the construction of a metamorphic field gradient that is composed of a continuum of rock quanta, each of which had a unique PT path. It is this interaction between deformation and metamorphism that produces the unusually steep metamorphic field gradients beneath ophiolites (Figure 11).

Figure 11 illustrates three end-member cases of accretion in thrust zones (introduced by Peacock [1987]) and the corresponding PT evolution of the base of the hangingwall of the thrust (i.e., in the position of an ophiolite sole). The assumption is made that the metamorphic field gradient approximates the peak metamorphic temperatures [England and Thompson, 1984, p. 936]. If no accretion occurs (Figure 11a), i.e., the subduction fault never changes position with respect to the hangingwall and footwall, then the rocks in the hangingwall simply cool during thrusting. The metamorphic field gradient reflects the thermal gradient at the initiation of faulting because that is when the temperatures were highest. If accretion is discontinuous (Figure 11b), i.e., a large slab of the underthrusting material accretes to the hangingwall as a single unit, then the metamorphic field gradient faithfully reflects the inverted thermal gradient that was present during thrusting. Continued thrusting results only in lower temperatures in the accreted rocks so that the metamorphic field gradient is unaffected. This type of accretion is only capable of producing inverted metamorphic field gradients like inverted thermal gradients, i.e., ~100 K km<sup>-1</sup>. A third type of accretion, continuous accretion (Figure 11c), is required to form the steep inverted metamorphic field gradients found beneath ophiolites. During continuous accretion a column of rock within the fault zone is built up from quanta of rocks that come from progressively greater distances up the fault zone.

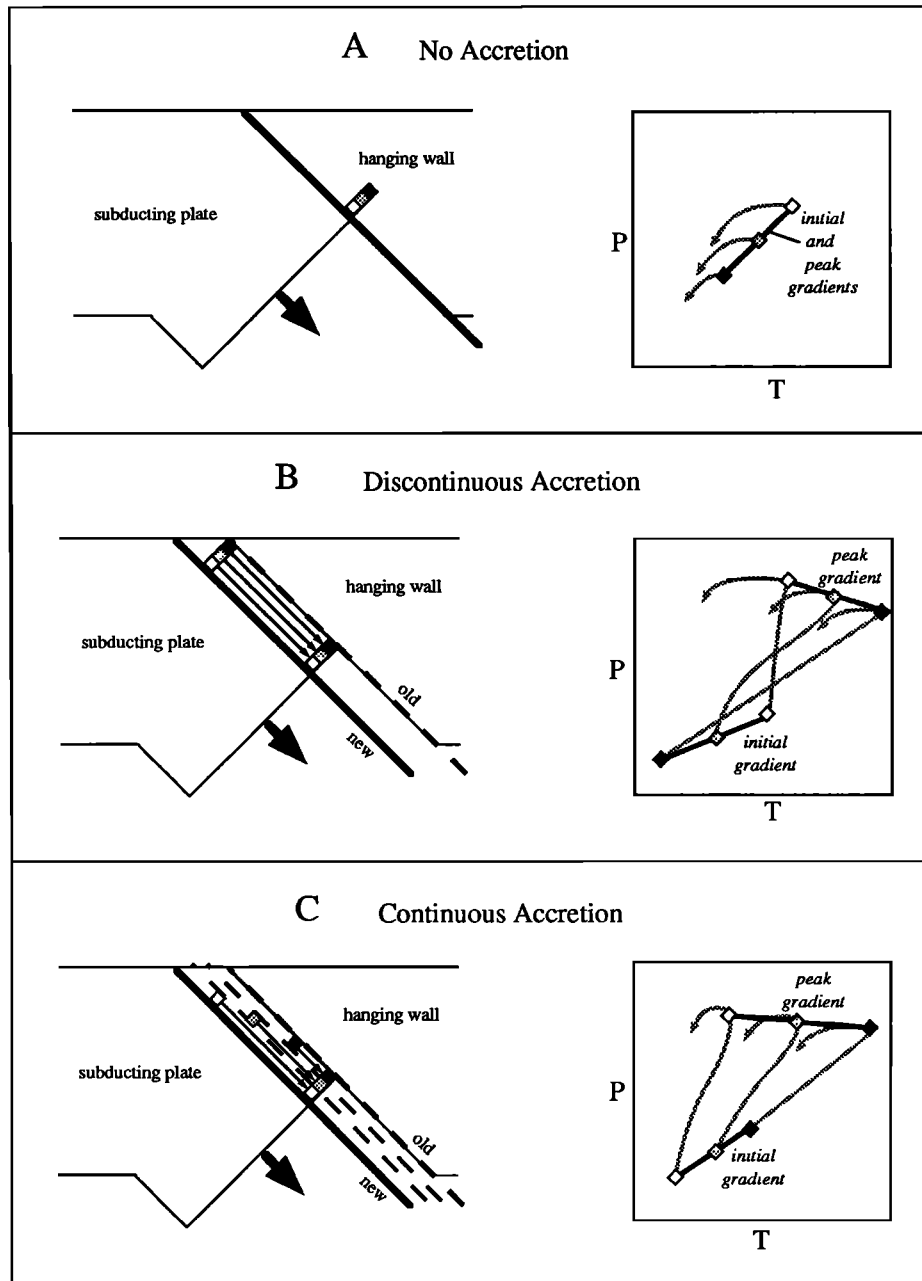


Fig. 11. Three end-member types of accretion in thrust zones. The cross sections (left) show a schematic subduction zone soon after faulting has begun. PT diagrams (right) illustrate PT evolution within the fault zone; gray lines delineate possible pressure-temperature paths, and black lines indicate initial and peak thermobarometric arrays. White, gray, and black squares in left and right frames correspond. (a) No accretion. Initial and peak gradients are identical, and an inverted metamorphic gradient does not develop. (b) Discontinuous accretion: the subduction fault jumps downward (from old to new position), accreting a piece of the footwall to the hangingwall. (c) Continuous accretion: the subduction fault moves progressively downward (from old to new via a continuum of intermediate positions), accreting pieces of the footwall to the hangingwall.

Consequently, as each quantum of rock arrives at its final destination where it accretes, the temperature at the accretion location may have changed significantly because of the additional time required to carry the quanta down the fault zone. Thus if cooling occurs, the inverted metamorphic field gradient is steeper than it would be if all the quanta accreted together (discontinuous accretion).

The pressures recorded at the peak temperatures (not necessarily the peak pressures) are distinctive for each type of accretion, as are the PT paths. For example, continuous accretion produces PT paths that do not cross (Figure 11c), whereas discontinuous accretion produces crossing PT paths (Figure 11b).

Tethyan-type ophiolites are an extreme example that a metamorphic field gradient need not reflect any particular thermal gradient that was present during the metamorphism [e.g., Spear and Selverstone, 1983]. This is true for regional metamorphic terranes because minerals in different portions of the metamorphic field gradient may have formed at different times. In Tethyan-type ophiolites, however, deformation plays an important role. The metamorphic field gradients in the metamorphic soles of Tethyan-type ophiolites are a sequence of rocks that were heated to different peak temperatures in disparate areas at different times and were amalgamated into a single column during subduction.

Thrust faulting is not the only type of faulting in which extreme metamorphic field gradients can develop. Unusual metamorphic field gradients could develop in the footwalls of normal fault zones where the heating hangingwall accretes to the uplifting, cooling footwall (the fault zone moves upward with time) (Figure 12). In such situations, absence of accretion preserves the initial metamorphic field gradient (Figure 12a), and discontinuous accretion leads to metamorphic field gradients that mimic the thermal gradients during the faulting, just like in thrust faults (Figure 12b). Continuous accretion, however, produces the reverse effect of thrust faults (Figure 12c). The metamorphic field gradient produced by continuous accretion during normal faulting is less steep than the thermal gradient during the metamorphism. This is because each quantum of rock accretes at a relatively higher temperature than it would during discontinuous accretion because the time required for the quantum to translate up the fault zone has allowed the hangingwall to reach higher temperatures.

Some thermobarometric studies of ophiolites indicate that the peak metamorphic pressures and temperatures decrease downward within the fault zone [e.g., Jamieson, 1986] (for an alternative view see El-Shazly and Coleman [1990]). Pavlis [1986] suggested that this downward decrease implies that the thrust system was rapidly exhumed or eroded during displacement. It is clear from the present study that such need not be the case. The downward decreasing pressure and temperature gradient can be formed by accretion of quanta of material from progressively shallower portions of the subduction zone.

## IMPLICATIONS

Many of the implications of this study are similar to those reported for earlier simulations of the evolution of the Oman

ophiolite sole [Hacker, 1990, pp. 4904–4906] based on the arc tectonic model of Lippard et al. [1986]. Several key results of this study based on the ridge tectonic model of Boudier and Coleman [1981] and Boudier et al. [1988] are different from the previous simulations and, furthermore, match the field observations in Oman more closely. Moreover, based on the simulations in this study, several predictions can be made that can be tested by further work in Oman.

1. Peak metamorphic temperatures recorded in the metamorphic sole should be greater at the leading edge of the ophiolite and lower at the trailing edge, because the entire system cooled with time and accretion began at the leading edge. There are no systematic measurements of the spatial variation in peak metamorphic temperatures in Oman. A useful field study would be to unravel the PT histories of rocks in the sole to determine the spatial distribution of peak temperatures and the shapes of PT paths. If the spatial variation predicted by the simulations can be found, then this study provides an explanation of how it might have developed. Furthermore, the spatial distribution of PT paths within the sole may yield clues about the geometry of emplacement, such as the distribution of heat within the lithosphere subducted beneath the ophiolite and the evolution of slab thicknesses.

2. The amphibolite-facies rocks in the Oman ophiolite sole should have been metamorphosed during a ~6–9 m.y. interval, although the duration of this metamorphism is related to the amount of oceanic lithosphere subducted beneath the ophiolite. The greatest shortcoming of the earlier simulations [Hacker, 1990] was that they indicated that the amphibolite-facies rocks formed in ~1–3 m.y., whereas the K/Ar ages indicate that the amphibolite-facies metamorphism in Oman spanned at least 7 m.y. [Alleman and Peters, 1972; Lanphere, 1981; Montigny et al., 1988]. Our current knowledge of the cooling ages of the sole comes solely from K/Ar dates on samples that are distributed somewhat erratically across the ophiolite and from samples whose structural and metamorphic relationships with surrounding rock units are incompletely documented. Moreover, the metamorphic petrogenesis of only a few of the dated samples have been thoroughly investigated. A major improvement in our current understanding would be to determine the cooling ages of the metamorphic sole using an isotopic system more informative than K/Ar, such as  $^{40}\text{Ar}/^{39}\text{Ar}$ . It is necessary that the metamorphic petrogeneses of the dated samples and their structural and metamorphic relationships with nearby rock units be carefully characterized. Comprehensive spatial distribution of samples from across the ophiolite exposure are also required to test the predictions of the simulations in this study.

3. Deformation within the sole should have occurred at maximum shear stresses of ~100 MPa. Molnar and England [1990] have made somewhat analogous calculations and concluded that thrusting along the Main Central Thrust in the Himalaya also occurred at shear stresses of ~100 MPa. Although stress magnitudes at some stages of the emplacement of the Oman ophiolite could possibly be estimated through microstructural paleopiezometry, such measurements have not yet been reported. Paleopiezometry of quartzite (present in the greenschist-facies portion of the sole) and dunite (present in the ultramafic tectonite) may

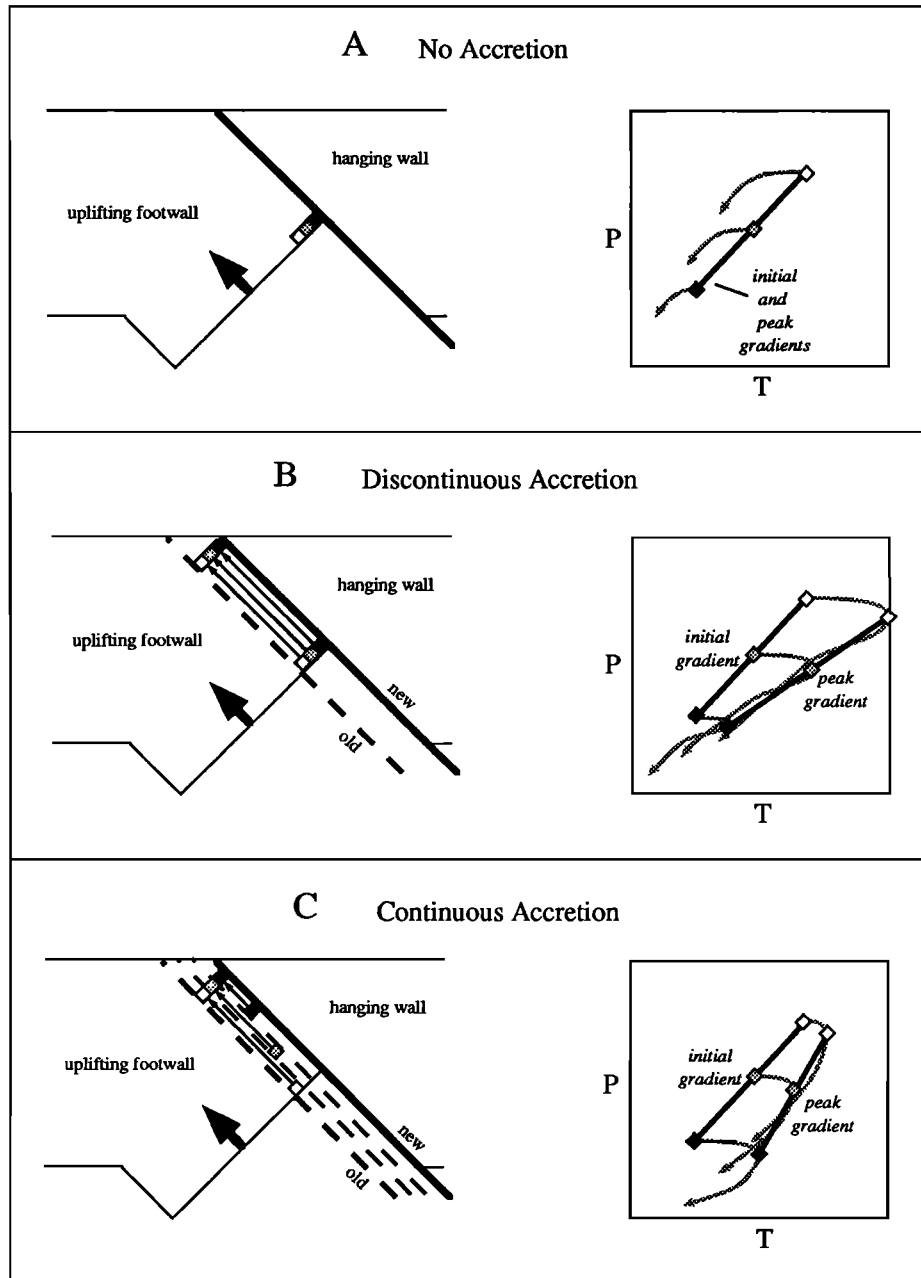


Fig. 12. Three end-member types of accretion in normal fault zones. PT diagrams illustrate PT evolution within the fault zone. The cross sections (left) show a schematic normal fault zone soon after faulting has begun. PT diagrams (right) illustrate PT evolution within the fault zone; gray lines delineate possible pressure-temperature paths, and black lines indicate initial and peak thermobarometric arrays. White, gray, and black squares in left and right frames correspond. (A) No accretion. Initial and peak gradients are identical. (B) Discontinuous accretion: the fault jumps upward (from old to new position), accreting a piece of the hangingwall to the footwall. (C) Continuous accretion: the subduction fault moves progressively upward (from old to new via a continuum of intermediate positions), accreting pieces of the hangingwall to the footwall.

provide some information about the stresses present during emplacement. Paleopiezometry can be difficult [e.g., Hacker et al., 1990], but recent information about quartz [Pierce, 1987; Pierce and Christie, 1987] and olivine [Karato, 1989] grain growth may assist in the interpretation.

4. The oceanic lithosphere was very young, probably <2 m.y. old. The age of the Oman lithosphere is not yet well constrained. U/Pb dates in plagiogranite bodies [Tilton et al., 1981] overlap K/Ar ages of the sole rocks [e.g., Montigny et al., 1988]. Sm-Nd dates on three gabbro samples [ $100 \pm 20$ ,  $128 \pm 20$ , and  $150 \pm 40$  Ma; McCulloch et al., 1981] have uncertainties that are too large to confirm or reject this prediction. A much-needed constraint on the tectonic evolution of the Oman ophiolite will come by determining the crystallization age of the gabbro, dikes, and/or lavas more precisely, perhaps by  $^{40}\text{Ar}/^{39}\text{Ar}$  or U/Pb dating as has successfully been employed in the Bay of Islands ophiolite by Dunning and Krogh [1985].

The Bay of Islands ophiolite is a Tethyan-type ophiolite exposed in the Canadian Appalachians. The inverted metamorphic field gradient in its sole has even higher peak temperatures than the Oman sole [Jamieson, 1986]. Unless another heat source is involved, the simulations presented here suggest that the Bay of Islands ophiolite also was very young when intraoceanic thrusting began. Early radiometric studies of the ophiolite plutonic section and sole [Dallmeyer and Williams, 1975; Archibald and Farrar, 1976; Mattinson, 1976; Jacobsen and Wasserburg, 1979] suggested that ~35 m.y. separated the igneous genesis of the ophiolite and its emplacement. More recent, higher precision U/Pb work [Dunning and Krogh, 1985] has narrowed the gap to only ~11–16 m.y. This is in accord with the prediction of this study that the amphibolite-facies metamorphism in the sole could continue for ~6–9 m.y. after intraoceanic thrusting of a very young ophiolite.

## CONCLUSIONS

The production and accretion of metamorphic rocks at the base of Tethyan ophiolites can be explained in terms of a physical model incorporating laboratory measurements of rheological and thermal properties. The temperature, stress, rock type, and displacement fields during ophiolite emplacement were modeled to understand the interaction between deformation and metamorphism. The metamorphic rocks are produced because cool basaltic rocks are subducted beneath warmer peridotite; they accrete to the base of the ophiolite because the sole thrust propagates downward from the peridotite into the basaltic rocks in response to the downward conduction of heat. The differential stress supported by basaltic material in the fault zone was of the order of 100 MPa (50 MPa maximum shear stress). The oceanic lithosphere subducted beneath the Oman ophiolite was probably very young (<2 m.y. old) as suggested by the peak metamorphic temperatures and K-Ar ages of the amphibolite-facies rocks of the sole thrust. The unusual metamorphic field gradients in the soles of Tethyan-type ophiolites are a sequence of rocks developed at different pressures and temperatures in disparate areas at different times that were amalgamated into a single column. Unusual

metamorphic field gradients may form in other tectonic settings, such as core complexes, where metamorphism and faulting are synchronous.

*Acknowledgments.* This paper is dedicated to Tucker "Bob" Wenzel. The manuscript benefitted from reviews by R. G. Coleman, W. G. Ernst, J. Karson, J. S. Pallister, and A. K. El-Shazly. Partial support was provided by DOE grant DE-FG03-87ER B806 to W. G. Ernst.

## REFERENCES

- Alabaster, T., J. A. Pearce, and J. Malpas, The volcanic stratigraphy of the Oman ophiolite complex, *Contrib. Mineral. Petrol.*, **81**, 168-183, 1982.
- Alleman, F. and T. Peters, The ophiolite-radiolarite belt of the North Oman Mountains, *Eclogae. Geol. Helv.*, **65**, 657-697, 1972.
- Archibald, D. A., and E. Farrar, K-Ar ages of amphibolites from the Bay of Islands ophiolite and the Little Port Complex, western Newfoundland, and their geological implications. *Can. J. Earth Sci.*, **13**, 520-529, 1976.
- Béchenec, F., J. Le Metour, D. Rabu, M. Villey, and M. Beurrier, The Hawasina basin: A fragment of a starved passive continental margin, thrust over the Arabian platform during obduction of the Semail nappe, *Tectonophysics*, **151**, 323-343, 1988.
- Blendinger, W., A. van Vliet, M. W. Hughes Clark, Uplifting, rifting and continental margin development during the Late Paleozoic in northern Oman, *Geol. Soc. Spec. Publ. London*, **49**, 27-37, 1990.
- Boudier, F., and R. G. Coleman, Cross section through the peridotite in the Samail ophiolite, southeastern Oman Mountains, *J. Geophys. Res.*, **86**, 2573-2592, 1981.
- Boudier, F., and A. Michard, Oman ophiolites the quiet obduction of oceanic crust, *Terra Cognita*, **1**, 109-118, 1981.
- Boudier, F., and A. Nicolas, (Eds.), The Ophiolites of Oman, special issue, *Tectonophysics*, **151**, 1-401, 1988.
- Boudier, F., G. Ceuleneer, and A. Nicolas, Shear zones, thrusts and related magmatism in the Oman ophiolite: Initiation of thrusting on an oceanic ridge, *Tectonophysics*, **151**, 275-296, 1988.
- Boudier, F., J. L. Bouchez, A. Nicolas, N. Cannat, G. Ceuleneer, M. Misseri, and R. Montigny, Kinematics of oceanic thrusting in the Oman ophiolite; model of plate convergence, *Earth Planet. Sci. Lett.* **75**, 215-222, 1985.
- Bratt, S. R., E. A. Bergman, and S. C. Solomon, Thermoelastic stress: How important as a cause of earthquakes in young oceanic lithosphere?, *J. Geophys. Res.*, **90**, 10,249-10,260, 1985.
- Casey, J. F., and J. F. Dewey, Initiation of subduction zones along transform and accreting plate boundaries, triple-junction evolution, and forearc spreading centres— Implications for ophiolite geology and obduction, in *Ophiolites and Oceanic Lithosphere*, edited by I. G. Gass, S. J. Lippard, and A. W. Shelton, *Geol. Soc. Spec. Publ., London*, **13**, 269-290, 1984.
- Ceuleneer, G., A. Nicolas, and F. Boudier, Mantle flow

- patterns at an oceanic spreading center: The Oman peridotites record, *Tectonophysics*, *151*, 1-26, 1988.
- Christensen, N. I., and J. D. Smewing, Geology and seismic structure of the northern section of the Oman ophiolite, *J. Geophys. Res.*, *86*, 2545-2555, 1981.
- Coleman, R. G., Tectonic setting for ophiolite obduction in Oman, *J. Geophys. Res.*, *86*, 2497-2508, 1981.
- Coleman, R. G. and C. A. Hopson, (Eds.), The Oman Ophiolite, *J. Geophys. Res.*, *86*, 2495-2782, 1981.
- Coney, P. J., and S. J. Reynolds, Cordilleran Benioff zones, *Nature*, *270*, 403-406, 1977.
- Cooper, D. J. W., Structure and sequence of thrusting in deep-water sediments during ophiolite emplacement in the south-central Oman Mountains, *J. Struct. Geol.*, *10*, 473-485, 1988.
- Dallmeyer, R. D., and H. Williams,  $^{40}\text{Ar}/^{39}\text{Ar}$  ages for the Bay of Islands metamorphic aureole: Their bearing on the timing of Ordovician ophiolite obduction. *Can. J. Earth Sci.*, *12*, 1685-1690, 1975.
- Dunning, G. R., and T. E. Krogh, Geochronology of ophiolites of the Newfoundland Appalachians. *Can. J. Earth Sci.*, *22*, 1659-1670, 1985.
- El-Shazly, A. K. and R. G. Coleman, Metamorphism in the Oman Mountains in relation to the Semail ophiolite emplacement, *Geol. Soc. Spec. Publ. London.*, *49*, 473-493, 1990.
- England, P. C. and A. B. Thompson, Pressure-temperature-time paths of regional metamorphism II. Their inference and interpretation using mineral assemblages in metamorphic rocks, *J. Petrol.*, *25*, 929-955, 1984.
- Ernewein, M., C. Pflumio, and H. Whitechurch, The death of an accretion zone as evidenced by the magmatic history of the Sumail ophiolite (Oman), *Tectonophysics*, *151*, 247-274, 1988.
- Gass, I. G., A. C. Ries, R. M. Shackleton, and J. D. Smewing, Tectonics, geochronology and geochemistry of the Precambrian rocks of Oman., *Geol. Soc. Spec. Publ. London*, *49*, 585-599, 1990.
- Ghent, E. D. and M. Z. Stout, Metamorphism at the base of the Samail ophiolite, southeastern Oman Mountains, *J. Geophys. Res.*, *86*, 2557-2571, 1981.
- Glennie, K. W., M. G. A. Boeuf, M. W. Hughes-Clark, M. Moody-Stuart, W. F. H. Pilar, and B. M. Reinhardt, Geology of the Oman Mountains, *Verh. K. Ned. Geol. Mijnbouwkd. Genoot. Ged. Ser.* *31*, 423, 1974.
- Hacker, B. R., Simulation of the metamorphic and deformational history of the metamorphic sole of the Oman ophiolite, *J. Geophys. Res.*, *95*, 4895-4907, 1990.
- Hacker, B. R., A. Yin, J. M. Christie, A. W. Snoke, Differential stress, strain rate, and temperatures of mylonitization in the Ruby Mountains, Nevada: Implications for the rate and duration of uplift. *J. Geophys. Res.*, *95*, 8569-8580, 1990.
- Harrison, T. M., Diffusion of  $^{40}\text{Ar}$  in hornblende, *Contrib. Mineral. Petrol.*, *78*, 324-331, 1981.
- Jacobsen, S. B., and G. J. Wasserburg, Nd and Sr isotopic study of the Bay of Islands ophiolite complex and the evolution of the source of mid-ocean ridge basalts. *J. Geophys. Res.*, *84*, 7429-7445, 1979.
- Jamieson, R. A., P-T paths from high temperature shear zones beneath ophiolites. *J. Metamorph. Geol.*, *4*, 3-22, 1986.
- Karato, S., Grain growth kinetics in olivine aggregates, *Tectonophysics*, *168*, 255-273, 1989.
- Kusznir, N. J., Thermal evolution of the oceanic crust; its dependence on spreading rate and effect on crustal structure, *Geophys. J. R. Astron. Soc.*, *61*, 167-181, 1980.
- Lanphere, M. A. K-Ar ages of metamorphic rocks at the base of the Semail ophiolite, Oman, *J. Geophys. Res.*, *86*, 2777-2782, 1981.
- Lipman, P. W., H. J. Protska, and R. L. Christiansen, Evolving subduction zones in the western United States, as interpreted from igneous rocks, *Science*, *174*, 821-825, 1971.
- Lippard, S. J., A. W. Shelton, and I. G. Gass, The ophiolites of northern Oman, *Mem. Geol. Soc. London*, *11*, 1-178, 1986.
- Manghnani, M. H. and R. G. Coleman, Gravity profiles across the Samail ophiolite, *J. Geophys. Res.*, *86*, 2509-2525, 1981.
- Mattinson, J. M., Ages of zircons from the Bay of Islands ophiolite complex, western Newfoundland. *Geology*, *4*, 393-394, 1976.
- McCulloch, M. T., R. T. Gregory, G. J. Wasserburg, and H. P. Taylor, Jr., Sm-Nd, Rb-Sr, and  $^{18}\text{O}/^{16}\text{O}$  isotopic systematics in an oceanic crustal section: Evidence from the Samail Ophiolite, *J. Geophys. Res.*, *86*, 2721-2735, 1981.
- Molnar, P., and P. England, Temperatures, heat flux, and frictional stress near major thrust faults, *J. Geophys. Res.*, *95*, 4833-4856, 1990.
- Montigny, R., O. Le Mer, R. Thuizat, and H. Whitechurch, K-Ar and  $^{40}\text{Ar}/^{39}\text{Ar}$  study of the metamorphic rocks associated with the Oman ophiolite, *Tectonophysics*, *151*, 345-362, 1988.
- Moores, E. M., Origin and emplacement of ophiolites, *Rev. Geophys.*, *20*, 735-760, 1982.
- Morgan, P., The thermal structure and thermal evolution of the continental lithosphere, *Phys. Chem. Earth*, *15*, 107-193, 1984.
- Morton, J. L., and N. H. Sleep, A mid-ocean ridge thermal model: Constraints on the volume of axial hydrothermal heat flux, *J. Geophys. Res.*, *90*, 11,345-11,353, 1985.
- Nicolas, A., F. Boudier, and J. L. Bouchez, Interpretation of peridotite structures from ophiolitic and oceanic environments, *Am. J. Sci.*, *280A*, 192-210, 1980.
- Nicolas, A., G. Ceuleneer, F. Boudier, and M. Misseri, Structural mapping in the Oman ophiolites: Mantle diapirism along an oceanic ridge, *Tectonophysics*, *151*, 27-55, 1988.
- Pallister, J. S., Structure of the sheeted dike complex of the Samail ophiolite near Ibra, Oman. *J. Geophys. Res.*, *86*, 2661-2672, 1981.
- Pallister, J. S., and R. T. Gregory, Composition of Samail oceanic crust, *Geology*, *11*, 638-642, 1983.
- Pallister, J. S., and C. A. Hopson, Samail ophiolite plutonic suite: Field relations, phase variation, cryptic variation and layering, and a model of a spreading ridge magma chamber, *J. Geophys. Res.*, *86*, 2673-2645, 1981.
- Pallister, J. S., J. C. Cole, D. B. Stoesser, and J. E. Quick, Use and abuse of crustal accretion calculations, *Geology*, *18*, 35-39, 1990.
- Parsons, B. P., and J. G. Sclater, An analysis of the variation of

- ocean floor bathymetry and heat flow with age, *J. Geophys. Res.*, **82**, 803-827, 1971.
- Pavlis, T.L., The role of strain heating in the evolution of megathrusts, *J. Geophys. Res.*, **91**, 12,407-12,422, 1986.
- Peacock, S. M., Creation and preservation of subduction-related inverted metamorphic gradients, *J. Geophys. Res.*, **92**, 12,763-12,781, 1987.
- Pearce, J. A., T. Alabaster, A. W. Shelton, and M. P. Searle, The Oman ophiolite as a Cretaceous arc-basin complex: Evidence and implications, *Philos. Trans. R. Soc. London, Ser. A*, **300**, 299-317, 1981.
- Penrose Conference Participants, Penrose field conference on ophiolites, *Geotimes*, **17**, 24-25, 1972.
- Pierce, M. L., Kinetics of recovery and grain growth in hydrostatically annealed quartz aggregates, M. S. thesis, 116 pp., Univ. of Calif., Los Angeles, 1987.
- Pierce, M. L., and J. M. Christie, Kinetics of grain growth in quartz aggregates, *Eos Trans. AGU*, **68**, 422, 1987.
- Robertson, A. H. F. and M. P. Searle, The northern Oman Tethyan continental margin: stratigraphy, structure, concepts and controversies. *Geol. Soc. Spec. Publ. London*, **49**, 3-25, 1990.
- Robertson, A. H. F. and N. H. Woodcock, Genesis of the Batinah mélange above the Semail ophiolite, Oman, *J. Struct. Geol.* **5**, 1-17, 1983a.
- Robertson, A. H. F. and N. H. Woodcock, Zabyat Formation, Semail Nappe, Oman: Sedimentation on to an emplacing ophiolite, *Sedimentology*, **30**, 105-116, 1983b.
- Robertson, A. H. F., C. D. Blome, D. W. J. Cooper, A. E. S. Kemp, and M. P. Searle, Evolution of the Arabian continental margin in the Dibba Zone, northern Oman Mountains. *Geol. Soc. Spec. Publ. London*, **49**, 251-284, 1990a.
- Robertson, A. H. F., M. P. Searle, and A. C. Ries (Eds.), The Geology and Tectonics of the Oman Region. *Geol. Soc. Spec. Publ. London*, **49**, 845 pp., 1990b.
- Sacks, I. S., The subduction of young lithosphere, *J. Geophys. Res.*, **88**, 3355-3366, 1983.
- Searle, M. P., The Haybi complex, northern Oman Mountains: Evidence for subduction - obduction and thrust emplacement processes beneath the Semail ophiolite, paper presented at Symposium on Ophiolite Genesis and Evolution of Oceanic Lithosphere, UNESCO-Sultan Qaboos University, Muscat, Oman, January 7-18, 1990.
- Searle, M. P., and J. Malpas, Structure and metamorphism of rocks beneath the Semail ophiolite of Oman and their significance in ophiolite obduction, *Trans. R. Soc. Edinburgh Earth Sci.*, **71**, 247-262, 1980.
- Searle, M. P., and J. Malpas, Petrochemistry and origin of sub-ophiolitic metamorphic and related rocks in the Oman Mountains, *J. Geol. Soc. London*, **139**, 235-248, 1982.
- Searle, M. P., S. J. Lippard, J. D. Smewing, and D. C. Rex, Volcanic rocks beneath the Semail ophiolite nappe in the northern Oman Mountains and their significance in the Mesozoic evolution of the Tethys, *J. Geol. Soc. London*, **137**, 589-604, 1980.
- Shelton, A. W., The interpretation of gravity data in Oman: constraints on the ophiolite emplacement mechanism. *Geol. Soc. Spec. Publ. London*, **49**, 459-471, 1990.
- Spear, F. S., and S. M. Peacock, Metamorphic Pressure-Temperature-Time Paths. *Short Course*, **7**, 102 pp., AGU, Washington, D.C., 1989.
- Spear, F. S. and J. Selverstone, Quantitative P-T paths from zoned minerals: Theory and tectonic applications, *Contrib. Mineral. Petrol.*, **83**, 348-357, 1983.
- Thomas, V., J. P. Pozzi, and A. Nicolas, Paleomagnetic results from Oman ophiolites related to their emplacement, *Tectonophysics*, **151**, 297-321, 1988.
- Tilton, G. R., C. A. Hopson, and J. E. Wright, Uranium-lead isotopic ages of the Semail ophiolite, Oman, with applications to Tethyan ocean ridge tectonics, *J. Geophys. Res.*, **86**, 2763-2775, 1981.
- Turcotte, D. L., W. F. Haxby, and J. R. Ockendon, Lithospheric instabilities, *Island Arcs Deep Sea Trenches and Back-Arc Basins, Maurice Ewing Ser.*, vol. 1, edited by M. Talwani and W. C. Pitman, AGU, Washington, D. C., 1977.
- Woodcock, N. H. and A. H. F. Robertson, The upper Batinah Complex, Oman: Allochthonous sediment sheets above the Semail ophiolite, *Can. J. Earth Sci.*, **19**, 1635-1656, 1982a.
- Woodcock, N. H. and A. H. F. Robertson, Stratigraphy of the Mesozoic rocks above the Semail ophiolite, *Geol. Mag.*, **119**, 67-76, 1982b.

---

B. Hacker, Department of Geology, School of Earth Sciences, Stanford University, Stanford, CA 94305-2115.

(Received August 31, 1990;  
revised December 4, 1990;  
accepted December 27, 1990.)